

Densification phenomena in the hot-pressing of spinel

R. J. BRATTON, G. R. TERWILLIGER, S. M. HO
Westinghouse Research Laboratories, Pittsburgh, Pennsylvania, USA

Hot-pressing of $MgAl_2O_4$ is examined at temperatures of 1300 to 1800°C and pressures of 141 to 352 kg/cm². The simple relationship $\ln P/P_0 = -Kt$ is used to characterize the hot-pressing behaviour. A transition occurs from an initial to an intermediate stage of densification, which depends more on time than on porosity. A final stage is associated with a decreased densification rate and begins when a significant change occurs in microstructure. A transition in the stress dependence of the intermediate region is indicative of a change in the densification mechanism at high stress. The activation energy for the intermediate stage of densification is 91.5 kcal/mol.

1. Introduction

Direct studies that tried to sort out the different variables affecting hot-pressing and to relate them to known hot-pressing models have been done for a number of oxides (e.g. MgO [1-3], BeO [1, 4], Al_2O_3 [5-10] and SiO_2 [11]). These have demonstrated that hot-pressing is not a simple process which occurs by a single mechanism over the full range of the variables, time, temperature, stress and microstructure. The initial stage of hot-pressing is often characterized by particle rearrangement, whereas the intermediate stage is characterized by plastic flow, viscous flow, or Nabarro-Herring diffusional creep. The same mechanisms used to explain intermediate stage hot-pressing are used to explain the final stage, but there are additional complications due to an increased driving force from surface tension of small pores or to grain growth causing either pore entrapment or coalescence. These phenomena and the mechanisms of hot-pressing have been discussed in detail by Spriggs [12] and Coble [13].

For $MgAl_2O_4$ spinel, statistical correlations between the densification behaviour and the hot-pressing variables have been reported for the temperature range 1170 to 1460°C [14]. This previous study indicated that the densification rate is nearly linear with the applied stress and has an activation energy of 87.5 kcal/mol for relative porosities $P \leq 0.15$. At higher temperatures, the stress dependence tended to increase.

In the present study, we extended the temperature range of hot-pressing of spinel to 1800°C and found that a simple equation revealed the significant features of the hot-pressing behaviour and allowed most of the phenomenon to be interpreted without going to a complex model.

2. Experimental procedure

2.1. Powder preparation

Powders of $MgAl_2O_4$ spinel were prepared from Linde A alumina (0.3 μm particle size) and reagent grade $Mg(NO_3)_2 \cdot 6H_2O$. The alumina was mixed to form a slurry with the nitrate solution, dried, and calcined at 600°C. Firing at 1400°C for 4 h produced completely reacted powder (confirmed by X-ray diffraction). Subsequent milling produced an average particle size of 0.4 μm .

2.2. Hot-pressing procedure

A sufficient amount of reacted powder was used to yield a 2.5 cm long pellet when hot pressed in a 2.5 cm i.d. graphite mould. The mould was inductively heated with an argon cover gas to prevent oxidation. For hot-pressing, a standard procedure was used of increasing the temperature and pressure in predetermined increments to the desired equilibrium temperature and pressure. When equilibrium was reached, the compaction of the specimens was measured with a dilatometer capable of determining movements of 0.0005 in. (0.00125 cm). Most of these isothermal

TABLE I Relative densities during hot-pressing trials at 352 kg/cm²

Time (min)	Relative density					
	1300°C	1400°C	1500°C	1600°C	1700°C	1800°C
5	0.691	0.781	0.945	0.977	0.9915	0.9946
10	0.650	0.820	0.952	0.983	0.9918	0.9954
15	0.672					
20	0.687	0.857	0.964	0.990	0.9931	0.9965
25	0.697	0.870	0.970	0.992	0.9938	
30	0.708	0.882	0.974	0.9941	0.9945	
60	0.746	0.923	0.989	0.9954	0.9957	
90	0.765					
120	0.777	0.964	0.993	0.9963	0.9964	
150	0.787					
180	0.805	0.983	0.994	0.9963	0.9967	

TABLE II Relative densities during hot pressing trials at different stresses

Time (min)	Relative density				
	1400°C			1500°C	
	141 kg/cm ²	211 kg/cm ²	282 kg/cm ²	141 kg/cm ²	247 kg/cm ²
5	0.618	0.697	0.736	0.7477	0.8986
10	0.641	0.723	0.757	0.7821	0.9255
15	0.656	0.746	0.777	0.8161	0.9553
20	0.670	0.762	0.788	0.8352	0.9710
25	0.681	0.774	0.806	0.8526	0.9799
30	0.691	0.783	0.817	0.8683	0.9848
60	0.735	0.826	0.861	0.9238	0.9914
90	0.758	0.859	0.887	0.9624	0.9919
120	0.775	0.879	0.906	0.9820	0.9919
150	0.788	0.894	0.921	0.9881	0.9919
180	0.797	0.904	0.932	0.9897	0.9919

hot-pressing tests were made for 3 h, but certain tests were terminated so that grain growth as a function of time could be determined.

After hot-pressing, the final density (ρ_f) of the compact was measured by water immersion and the density at any time (ρ_t) was determined simply by the equation

$$\rho_t = \rho_f \frac{L_f}{L_t} \quad (1)$$

where L_f is the final length of the compact and L_t is the length at any time, t , determined from the movement of the dial gauge and L_f .

For microstructure examination, the hot-pressed specimens were polished and etched 10 min in boiling phosphoric acid. Grain sizes of the specimens were determined by standard intercept and comparison methods.

3. Results

The determined relative densities (ρ_t/ρ_{th} ; $\rho_{th} =$

3.58 g/cm³, theoretical density of spinel) are given in Tables I and II for the various temperatures and stresses studied. Grain sizes resulting from different hot-pressing conditions are given in Table III.

4. Discussion

We chose to analyse our results according to the equation

$$\ln P/P_0 = -Kt \quad (2)$$

where P is the relative porosity ($P = 1 - \rho_t/\rho_{th}$) at time t , P_0 is the initial relative porosity, and K is a constant which is a function of stress, temperature, and microstructure. Considerable discussion can be found in the literature as to the proper function for describing hot-pressing. Our reasons for using Equation 2 are:

1. Equation 2 is similar in form to the equations for the plastic flow model, the model derived from the Nabarro-Herring creep model [9] and to the phenomenological model of Rummeler and

Palmour [14].

2. Equation 2 follows first order kinetics, i.e. $(dP)/dt = -KP$, and therefore predicts that the rate of removal of porosity is proportional to the porosity present.

3. If hot-pressing is considered to consist of an initial, intermediate, and final stage, then Equation 2 produces consistent results with our data for the intermediate stage.

4. The equation is linear with our data over the intermediate stage of hot-pressing. Second order kinetics, other hot-pressing equations, and the correction of stress by various functions used to describe stress concentration by porosity, do not improve the fit to the data.

Fig. 1 is a plot of the data obtained at temperatures of 1300 to 1800°C for a stress of 352 kg/cm². Very high densities were quickly reached at temperatures above 1400°C. Fig. 2 shows the 1400°C data plotted according to Equation 2 and Fig. 3 shows the 1500°C data plotted the same way. At 1400°C, the fit is linear after about 30 min, and at 1500°C the fit is linear after about 10 min.

Rummler and Palmour [14] observed that a non-linear initial stage of densification occurred until $P \leq 0.15$. Our data show no distinct change at a certain porosity, and in fact, the data

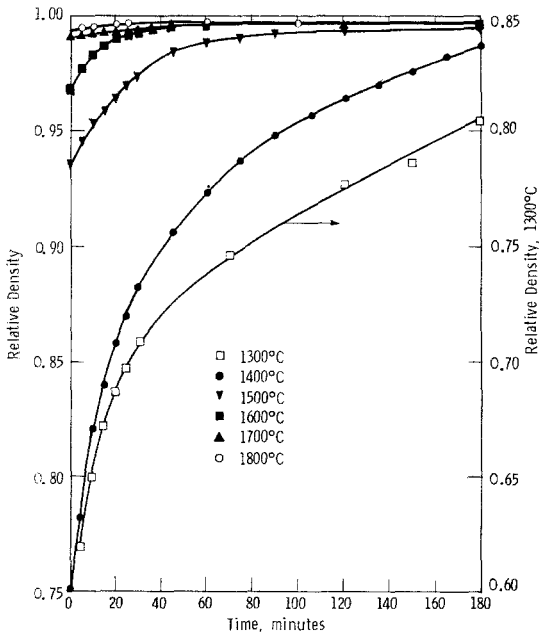


Figure 1 Spinel hot-pressing data at various temperatures at 5000 psi (352 kg/cm²).

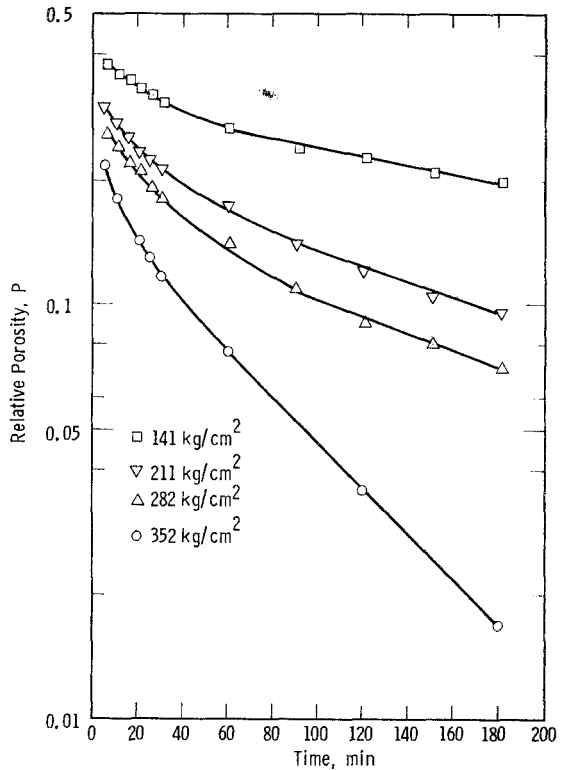


Figure 2 Spinel hot pressing data at 1400°C plotted according to the equation $\ln P/P_0 = -Kt$. The initial and intermediate stages are apparent.

are linear according to Equation 2 in certain cases up to $P = 0.27$. It appears that the duration of this initial stage depends as strongly on time as it does on porosity at a given temperature and pressure, and the point of transition between the initial densification region and the linear region cannot be identified with either pore closure or isolation as previously suggested.

For the linear region, the constant K in Equation 2 contains the stress dependence of the hot-pressing rate. Assuming a parabolic relationship, $K \propto \sigma^n$, and no interaction between stress and porosity, then n can be determined from Fig. 4. It is apparent from Fig. 4 that at 1400°C there is a change in the stress dependence over the range of stresses studied here. Below 282 kg/cm², $n = 1.26$, a value near to $n = 1$ which is indicative of Newtonian or "viscous" behaviour (indicating densification is proceeding by diffusional creep). However, it is also similar to 1.3 which was found for the creep of polycrystalline alumina and ascribed to grain-boundary sliding [15]. There are not sufficient data to determine

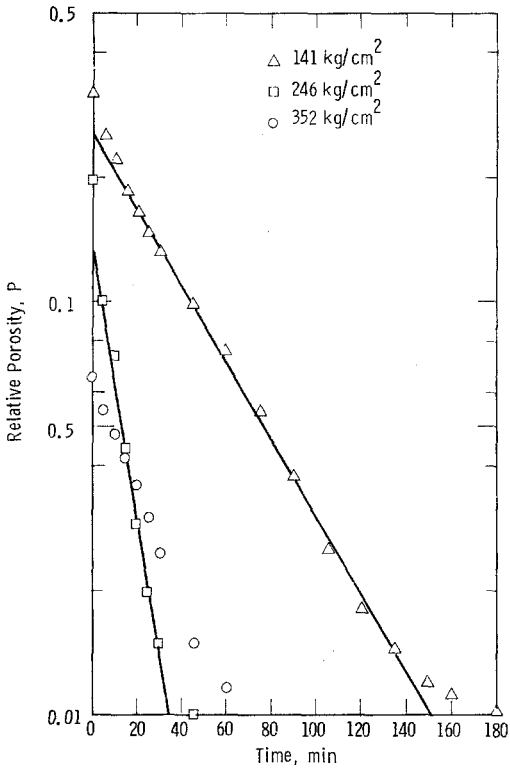


Figure 3 Spinel hot-pressing data at 1500°C plotted according to the equation $\ln P/P_0 = -Kt$. These data show a final densification stage.

if $n > 1$ because of a single mechanism or because the high stress mechanism is concurrently contributing to the densification at the low stresses. Above 282 kg/cm², $n = 3.83$ and there is definitely a distinctly different mechanism contributing to the densification. The value of n is in the range of n -values (3 to 5) derived for dislocation models of creep [16-19]. Higher applied stresses would probably give slightly higher values of n because the high stress mechanism would be completely dominant. It is interesting to note that in spite of the two different mechanisms above and below 282 kg/cm², Equation 2 fits the different data equally well at 1400°C.

The hot-pressing data at 1500°C are not as easily explained. These data show very little of the initial stage behaviour that was observed at the lower temperatures, and show a reduced rate of densification at low porosities, which was not found for the lower temperatures. A likely reason for the absence of an initial period at high temperatures is that by the time the equilibrium

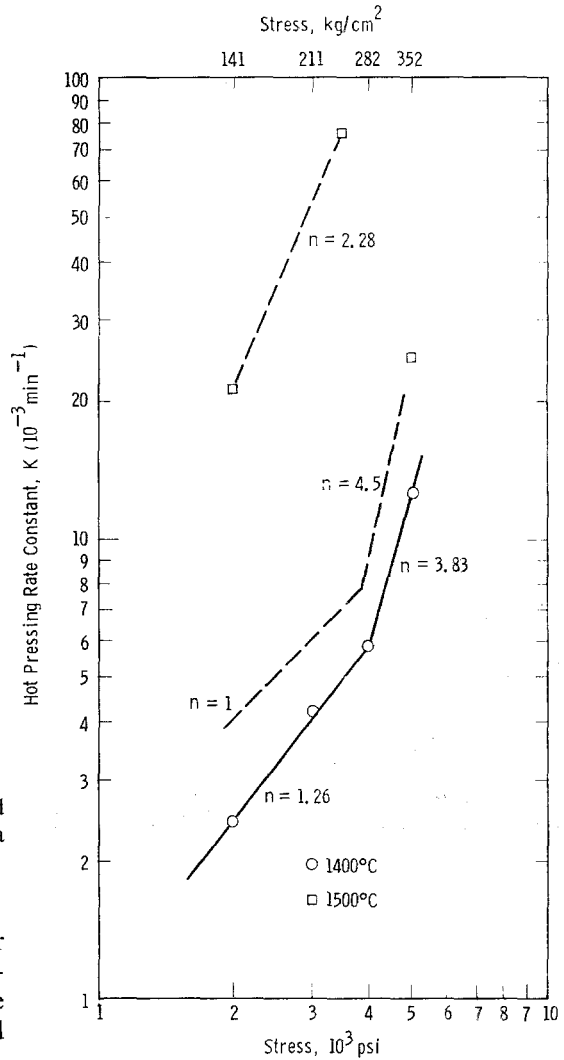


Figure 4 Stress dependence of the hot-pressing rate constant at 1400 and 1500°C.

temperature and stress are reached the specimen is quite dense and particle rearrangement is restricted due to particle bonding. Thus, the intermediate stage of densification, which is linear with respect to Equation 2, begins immediately.

A reduced rate of densification appears at longer times for the 1500°C data at 141 and 246 kg/cm². The 352 kg/cm² data are reduced over the full range of densification observed ($\rho_i/\rho_{th} > 0.93$). Likewise, the 1600 to 1800°C data are reduced over the observed range of densities of $\rho_i/\rho_{th} > 0.96$.

This reduction in the hot-pressing rate constant, K , signals a final stage densification.

during which significant changes in microstructure are occurring. Grain sizes in Table III indicate that measurable grain growth occurred at all temperatures above 1400°C. Grain size, d , approximated the relation $d^2 \sim t$, except at 1800°C, where the relation was closer to $d^4 \sim t$. Thus, the microstructures were changing significantly and this affected the densification rates. During grain growth, a pore on a boundary is either incorporated into the interior of a grain or swept along with the boundary. In the former case, the pore is isolated from the high diffusivity path of the boundary and its rate of shrinkage decreases. In the latter case, the pore is likely to coalesce with others and grow. Either case results in a decrease in the rate of densification and both were observed in the specimens hot-pressed in this study (see Fig. 5).

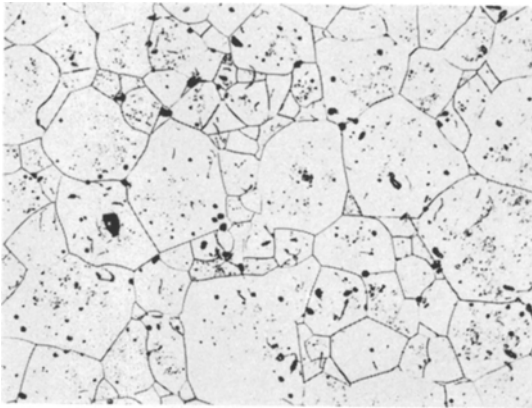


Figure 5 Microstructure of nearly dense spinel showing pores at triple points, at grain boundaries and within grains. Hot-pressed at 1800°C for 180 min ($\times 120$).

TABLE III Grain growth data for spinel at 352 kg/cm²

t (h)	Grain size (μm)			
	1500°C	1600°C	1700°C	1800°C
0.5	1.1	2.6	8.0	41.2
1.0	1.3	3.2	9.6	48.5
2.0	1.6	3.9	11.7	58.5
3.0	1.9	4.5	13.5	65.2

Another phenomenon which was apparent from the microstructures is the recrystallization of very large, straight-sided grains in the fine-grain matrix. This is illustrated in Fig. 6. It was most pronounced at the higher temperatures, but even at 1500°C the grain size distribution appears to be bimodal. A wide range of grain sizes

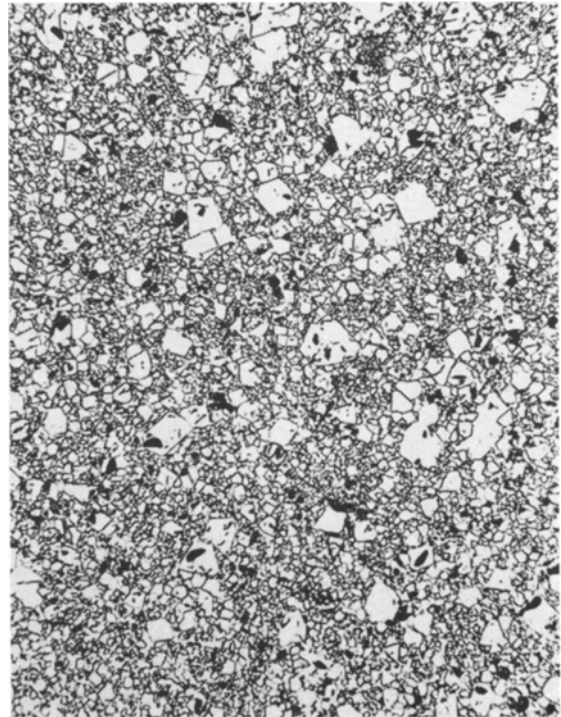


Figure 6 Recrystallization of large grains at 1700°C after 120 min ($\times 187$).

persisted even when the specimens were about completely dense and considerable grain growth had occurred, as shown in Fig. 5. The effect of this recrystallization and non-uniform grain size distribution on the rate of densification is not entirely clear. A large average grain size due to recrystallization is reasonably expected to decrease the rate of densification when it occurs by Nabarro-Herring creep. But since the most significant recrystallization occurred in the region of large n and a greater plasticity would be expected of the large recrystallized grains, the recrystallization phenomenon appears to slow densification only because it traps pores within grains and causes pore coalescence.

Further evidence that microstructural changes are modifying the densification process is given in the Arrhenius plot of K in Fig. 7. The low temperature, low stress data yield an activation energy of 91.5 kcal/mol which is close to that found by Rummeler and Palmour (87.5 kcal/mol) for hot-pressing and slightly lower than that found by Bratton [20] (118 kcal/mol) for the intermediate stage of sintering controlled by volume diffusion. At high temperatures (and

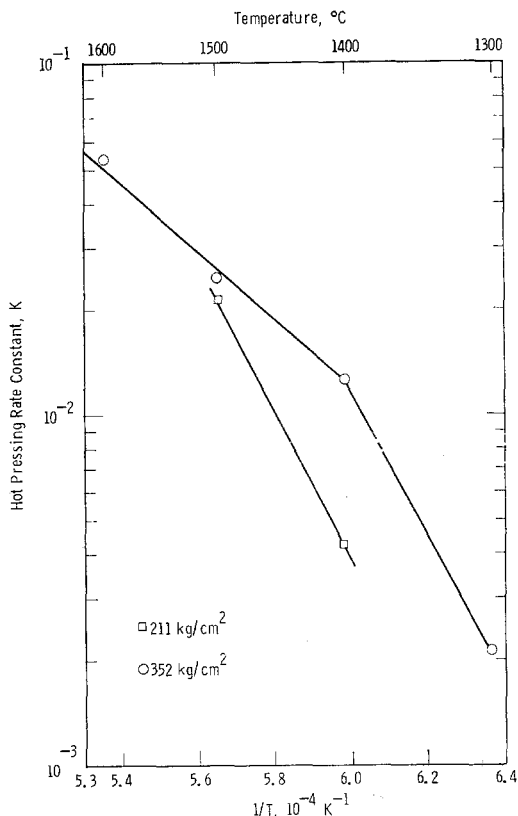


Figure 7 Arrhenius plot of the hot-pressing rate constant, K .

therefore low porosities), the activation energy for hot pressing is only 57.4 kcal/mol. This low activation energy is not indicative of the densification process in spinel; instead it means that the data cannot be compared on the basis of temperature alone because the microstructures are not constant at the higher temperatures.

Rummler and Palmour found that the activation energy for densification decreased continuously from 122 to 88 kcal/mol as P decreased from 0.25 to 0.02. In this study the activation energy was found to be invariant over the intermediate stage of hot-pressing, i.e. after the initial stage was complete and before the final stage began as signified by changes in the microstructure. This invariance is demonstrated by the linearity of Equation 2 over a large range of porosity $P \geq 0.07$.

5. Conclusions

The simple relationship $\ln P/P_0 = -Kt$ is useful for revealing the significant characteristics of the hot-pressing behaviour of MgAl_2O_4 spinel. This behaviour is characterized by an initial, intermediate, and final stage of densification. The point of transition between the initial and the intermediate stages depends more significantly on time than on porosity, and the final stage begins when significant changes in the microstructure occur. A transition in the stress dependence of the intermediate region is indicative of a change in the mechanism of densification at high stresses. An activation energy of 91.5 kcal/mol was found for the intermediate stage of densification.

References

1. P. MURRAY, E. P. RODGERS, and A. E. WILLIAMS, *Trans. Brit. Ceram. Soc.* **53** (1954) 474.
2. T. VASILOS and R. M. SPRIGGS, *J. Amer. Ceram. Soc.* **46** (1963) 493.
3. P. RAMAKRISHNAN, *Trans. Brit. Ceram. Soc.* **67** (1968) 135.
4. I. AMATO, R. L. COLOMBO, and M. RAVIZZA, *J. Nucl. Mater.* **22** (1967) 97.
5. G. E. MANGSEN, W. A. LAMBERTSON, and B. BEST, *J. Amer. Ceram. Soc.* **43** (1960) 55.
6. E. J. FELTEN, *ibid* **44** (1961) 381.
7. R. L. COBLE and J. S. ELLIS, *ibid* **46** (1963) 438.
8. T. VASILOS and R. M. SPRIGGS, *ibid* **48** (1965) 493.
9. R. C. ROSSI and R. M. FULRATH, *ibid* **46** (1965) 558.
10. G. M. FRYER, *Trans. Brit. Ceram. Soc.* **68** (1969) 185.
11. T. VASILOS, *J. Amer. Ceram. Soc.* **43** (1960) 517.
12. R. M. SPRIGGS, "High Temperature Oxides, Part III, Magnesia, Alumina, Beryllia Ceramics: Fabrication, Characterization and Properties", ed. A. M. Alper (Academic Press, New York, 1970) p. 183.
13. R. L. COBLE, *J. Appl. Phys.* **41** (1970) 4798.
14. D. R. RUMMLER and H. PALMOUR, III, *J. Amer. Ceram. Soc.* **51** (1968) 320.
15. T. SUGITA and J. A. PASK, *ibid* **53** (1970) 609.
16. J. WEERTMAN, *J. Appl. Phys.* **26** (1955) 1213.
17. *Idem*, *ibid* **28** (1957) 362.
18. C. R. BARRETT and W. D. NIX, *Acta Metallurgica* **13** (1965) 1247.
19. F. R. N. NABARRO, *Phil. Mag.* **16** (1967) 231.
20. R. J. BRATTON, *J. Amer. Ceram. Soc.* **54** (1971) 141.

Received 1 May and accepted 13 June 1972.